Analyst

Accepted Manuscript

ROYAL SOCIETY OF CHEMISTRY

www.rsc.org/analyst

Analyst

RSCPublishing

COMMUNICATION

Composite SERS-based satellites navigated by optical tweezers for single cell analysis

Cite this: DOI: 10.1039/x0xx00000x

Received 00th February 2015,
Accepted 00th February 2015

DOI: 10.1039/x0xx00000x

www.rsc.org/

Inna Y. Stetciura,[a,b] Alexey Yashchenok,[a,c] Admir Masic,[c] Evgeny V. Lyubin,[d] Olga A. Inozemtseva,[a] Maria G. Drozdova,[e] Elena A. Markvichova,[e] Boris N. Khlebtsov,[f] Andrey A. Fedyanin,[d] Gleb B. Sukhorukov,[g] Dmitry A. Gorin*[a] and Dmitry Volodkin*[b]

Here we have designed composite SERS active micro-satellites possessing a dual role working as: i) effective probes for cellular composition and ii) optically movable and easily detectable markers. The satellites were synthesized by the layer-by-layer assisted decoration of silica microparticles with metal (gold or silver) nanoparticles and astralen in order to ensure satellite SERS-based microenvironment probing and satellite recognition, respectively. A combination of optical tweezers and Raman spectroscopy can be used to navigate the satellites to a certain cellular compartment followed by the cellular uptake and also to probe the intracellular composition. The developed approach may serve in future as a tool for the single cell analysis focusing on both extracellular and intracellular studies with nanometer precision due to the multilayer surface design.

The single cell analysis is nowadays an extremely developing and highly promising scientific field aiming at analysis of extracellular and intracellular composition up to the level of a single cell.[1] High heterogeneity of biological cells has stimulated a research towards biological analysis of a single cell.[2,3] Up to now the single cell analysis is fast being developed in applied fields such as diagnostics and biosensors. A number of different techniques applicable to the single cell analysis are rapidly growing including microfluidics that gives an option to separate biological cell and reduce analyzed volumes.[4,5]

SERS is a non-contact and label-free method already applied and having strong potential to reveal a composition of biological tissues in real-time.[6,7] The method has high sensitivity allowing us to detect of a single molecule[8] and approach the single cell analysis.[9] Up to now progress in SERS is limited by the development of new nanostructured materials which can be used as SERS platforms for biomedical applications. Generation of effective surface enhancement of Raman scattering was demonstrated by specially prepared metal surfaces with high roughness. Various types of rough metal surfaces were obtained by patterning[10-12] or multistage transfer printing[13] and nanoparticle assemblies made of gold nanorods,[14,15] nanostars,[16,17] mesoflowers,[18] silver nanorods,[19] nanowires[20] and core-shell nanoparticles[10]. Thanks to the great progress in synthesis of metal nanoparticles, one of the simplest and most cost-effective strategies to manufacture SERS platforms is to fabricate self-assembled nanoparticles. However, the limitations to use the nanoparticles are caused by their small sizes leading to great difficulties in their manipulation and detection. More importantly, accumulation of SERS signal from single nanoparticle still remains challenging.

In contrast, micrometer sized particles can be easily observed using an optical microscope. Moreover, it is also reported that microparticles of spherical shape can be easily moved with optical tweezers.[21-23] The layer-by-layer assembly method has already been applied to the formation of nanocomposite shells using SERS platforms.[24,25] The shells can be engulfed by a living cell allowing SERS based intracellular analysis.[26] However, as far as we know there are no studies demonstrating externally triggered positioning of SERS active platforms for localized cellular studies. Here for the first time we demonstrate

that optical tweezers can be used to position SERS active microspheres onto a surface of L929 mouse fibroblasts and the intracellular composition can be probed for the engulfed microspheres.

First, we synthesized composite microparticles to be used as SERS active satellites. As a solid support we chose silica microparticles because the particles are well suited for surface modification. The LbL assembly technique allows us to modify a surface of various solid particles to possess certain functionality.[27-29] We utilized this approach for making the satellites detectable by Raman spectroscopy. For this purpose a thin multilayer film (poly(allylamine hydrochloride)/astralen)$_3$ or (PAH/Astralen)$_3$ was deposited on the surface of solid silica microparticles (Fig. 1). Astralen serves as a marker easily detectable by Raman spectroscopy.[30] PAH is here a kind of "glue molecules" providing complexation of the astralen particles by the LbL manner to tailor astralen on the microparticle surface. Three bilayers were chosen to ensure enough molecules of astralen per particle surface.

At the next step the particles were modified by metal nanoparticles in order to create surface for effective enhancement of a Raman signal (Fig. 1). Both silver and gold nanoparticles as well as films made from these nanoparticles are known to be effective SERS coatings.[26,31] Silver or gold were chemically reduced to the surface by previously established protocols.[32] The composition of the core-shell microparticles was as follows: silica microparticles/(PAH/astralen)$_3$/Au(or Ag).

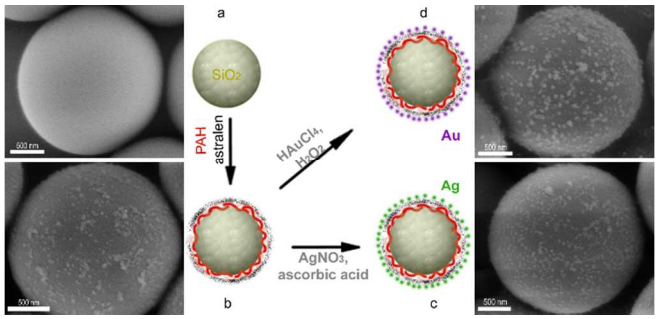

Fig. 1. The scheme of fabrication of SERS active satellites and corresponding SEM images at every fabrication step: a - SiO_2 microspheres, b - SiO_2/(PAH/Astralen)$_3$, c - SiO_2/(PAH/Astralen)$_3$/Ag and d- SiO_2/(PAH/Astralen)$_3$/Au microspheres.

SEM analysis clearly demonstrates an increase of the surface roughness after deposition of (PAH/astralen)$_3$ film as well as after the metal nanoparticles adsorption and subsequently their chemical reduction. The surface roughness of the microparticles after the deposition of the metal nanoparticles (Au or Ag) is in the range comparable with the sizes of probed molecules. This increase a chance to get strong enhancement of the Raman signal for the biomolecules located in the vicinity of the inhomogeneous metal surface. As shown in our previous study the deposition of (PAH/astralen)$_3$/Ag onto $CaCO_3$ microparticles leads to an effective enhancement of Raman signals of biomolecules (e.g. polylactide and hyaluronic acid) commonly used for tissue engineering applications.[32] However, in contrast to the silver particles the plasmon peak of the particles coated with gold is red-shifted. This allows using infrared laser range and thus to carry out non-invasive manipulation in a living tissue. Therefore, we tested the SERS activity of the satellites synthesized here for cellular experiments as will be shown later.

At the next step we have tested the capability of holding engineered microparticles by optical tweezers. The holding and subsequent moving were carried out by a continuous-wave diode infrared laser. Both types of the satellites (coated with silver or gold nanoparticles) were trapped by a focused laser beam. However, trapping of the gold-coated satellites was more effective because silver coated particles were escaped from a laser trap more often. We believe that this behavior deals with a low chemical stability of the silver coatings as compared with the gold ones.[33] Thus, the structure of the silica-based platforms with the gold coating was more effective providing stable capture by laser tweezers as schematically shown in Fig. 2a,b (see also video file in the Supporting information section). According to this scheme, the movement of the laser beam towards the glass substrate results in simultaneous moving of the captured satellites to the same direction. In the real cellular experiment the described movement leads to a clear visual observation of the cell (Fig. 2c-d).

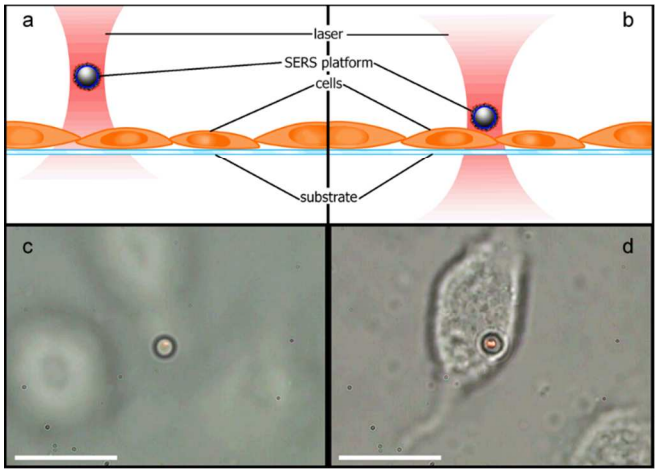

Fig. 2. Schematics of SERS active satellites trapping by laser tweezers to the surface of a cell (a-b). Optical transmission images of SERS active satellite trapped by tweezers above L929 mouse fibroblast cell (c) and in the vicinity of cell membrane (d). For movie see the Supporting information. Scale bars in optical images are 10 μm.

The cell is better focused when the satellite approaches the cellular surface. Upon contact of the satellite with the cellular surface the focused laser was off leading to sticking of the satellite to the cell surface. Thus, one can easily choose a position of interest on the cell surface with a micrometer precision and navigate the satellite to this position and subsequently release the satellite. The experiments with cells were carried out both in PBS buffer and in culture medium. In

both cases the SERS platforms were successfully taken and consistently held by the laser trap (see video in the Supporting information section). This demonstrates that the navigation by the optical tweezers can be performed under physiological conditions in the course of the real cellular experiment.

It is of interest to explore an intracellular environment by the satellites placed in contact with a certain cellular compartment. We found that after the contact with the cell surface the satellites were engulfed by a cell after four hours of incubation. This was proven by CLSM imaging using Z-stacking (Fig. 3). For this experiment the cells were stained by calcein according to the protocol elaborated earlier.[34] The red satellite (prepared using PAH-tetramethylrhodamine (PAH-TRITC)) can be easily recognized in the green-colored cell (Fig. 3b). The Z-stacking reconstruction profiles were obtained along two perpendicular lines (red and green), which went through the satellites and the cell. In spite of the fact that resolution of Z-stacking is not high enough compared to XY-plane scanning,[35] one can clearly see that the satellites were located next to the bottom of the glass but not on the cell top. This observation proves that the cells engulf the satellites after four hours of incubation.

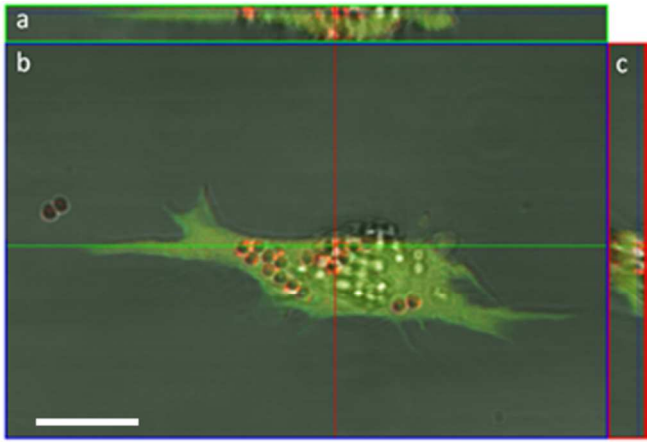

Fig. 3. (b) - CLSM image of L929 mouse fibroblast cell after 4 hours of incubation with SiO_2/(PAH-TRITC/Astralen)$_3$/Au particles. The cell has been staining by calcein (green color). (a) and (c) - reconstruction images made from Z-stacking of profiles obtained along the red and green lines on the image (b), respectively. Scale bar equals 20 μm.

The cytotoxicity analysis was performed by MTT technique. In the test a mouse fibroblast cell line L929 was used. The cells were cultivated in Dulbecco's modified Eagle medium (DMEM) supplemented with 10% FBS in culture flasks (25 cm^2) in a CO_2 incubator at 37°C in a humidified atmosphere containing 5% of CO2. To carry out MTT-test, the cells were seeded into 96-platees (10^4 cells/well) and exposed in CO_2 incubator in the presence of various SERS platforms for 24 hours. As seen in Fig.1, we did not observe any acute cytotoxicity in a range of SERS concentrations (about 1000-2000 particles/well) which were used in this study. The cell viability changing was not statistically significant compared to the control (monolayer culture without SERS platforms (Figure S2).

Following the navigation experiments we focused on the probing of the intracellular environment by the developed satellite. Before Raman experiments the cell culture medium was replaced by PBS buffer after cell cultivation for approximately 4 hours on a glass substrate. Afterwards Raman spectra were acquired from the satellite located inside the cell at laser power of 0.2 μW and irradiation wavelength of 785 nm. This extremely low power of the used IR laser ensures non-invasive Raman measurements.[36]

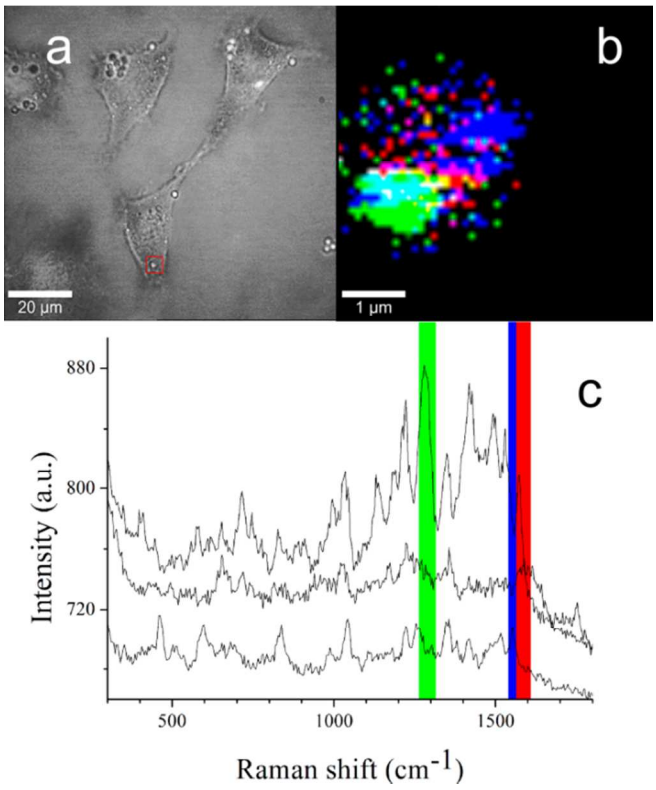

Fig. 4. a - Optical image of L929 mouse fibroblast cells after 4 hours of incubation with SiO_2/(PAH/Astralen)$_3$/Au satellites; b - Mapping of Raman signals coming from the area (red rectangle) depicted in the image (a) according to the chosen characteristic bands represented in the image (c). The characteristic bands of astralen (in red), DNA (in blue), and lipids (in green) are highlighted in the spectra (c). The spectra are taken at wavelength of 785 nm and power of 0.2 μW.

Fig. 4 shows the cells with uptaken satellites (a) including the enlarged image with the mapping of the area around the satellite (b). The Raman spectra (c) were taken and certain bands (green, red and blue) were chosen for mapping the enlarged cell image according to these bands (Fig. 4b). The signals in the spectra were coming from biologically relevant compounds as identified by colors according to the typical bands on the Raman spectra (Fig. 4b,c). The red area in Figure 4c corresponds to astralen[30] (typical C=C band oscillation in the range of 1500 − 1900 cm^{-1}). Astralen can be used as a marker in complex environments, such as biological fluids, living

tissues and cells.[32] Lipids are shown in green color (Figure 4c) that corresponds to the characteristic band of ~1656 cm^{-1} indicated the presence of C–C stretch vibrations, while the position of a band at 1740 cm^{-1} indicates the presence of carbonyl (C=O) stretching bands. In addition to lipids bands, the probe reveals peaks related to aromatic ring vibrations of nucleic acids, namely DNA/RNA macromolecules (bands at 1314 cm^{-1}, 1376 cm^{-1} and 1479 cm^{-1}), which were marked by blue color in Fig. 4b,c.

The two well-identified spots of blue and green colors show the distribution of nucleic acids and lipids near the satellite surface (Fig. 4b). One can speculate that the cell nucleolus is located on the right side of the satellite and the lipidic membrane on the left underneath the area of the satellite. This may happen because the size of the satellite (2 μm) is closed to the thickness of a spread cell and cellular compartments are expected to be in direct contact with the uptaken satellite. Thus, the satellites prepared in this study may be used for probing intracellular composition by Raman analysis. We believe that a combination of optical tweezers and Raman spectroscopy may open a way to the single cell analysis with high spatial and temporal precision focusing not only on the intracellular composition but also on highly dynamic extracellular microenvironment. Single cell analysis using LbL assembled films loaded with bioactive molecules gives many options for analysis of extracellular microenvironment.[37, 38] Externally controlled delivery from microcarriers embedded into the LbL films[39, 40] shows new opportunities for localized non-invasive delivery on demand. For this purpose, encapsulation of fragile biologically active molecules into externally activated containers such as LbL-assembled microcapsules should further be developed.[41,42] The issues considered above might be of great importance for tissue engineering applications and fundamental study of cell biology.

Conclusions

SERS active satellites with a multifunctional shell composed of Raman active compound (astralen) and electroless plating either Au or Ag nanoparticles assembled by the LbL technique were externally trapped by optical tweezers and located onto the surface of living L929 mouse fibroblasts with a micrometer precision. The satellites coming to contact with the cell surface were internalized by L929 mouse fibroblasts after 4 hours of incubation. It should be noted that it is possible to use the automatic movement of the laser trap[43], and thus SERS sensors, to given coordinates for increasing of the accuracy of satellite positioning in space. Astralen as a Raman tag in SERS satellite shell enables one to recognize a probe inside the cells. Probing the cellular internal composition by SERS satellite identifies characteristic cellular biomolecules such as nucleic acids and lipids.

Experimental Section

Materials. Poly(allylamine hydrochloride) (PAH, MW ~ 70000, Sigma, Aldrich), sodium hydroxide, tetrakis (hydroxymethyl) phosphonium chloride (THPC, Fluka), and potassium carbonate were purchased from Sigma-Aldrich (Germany). Sodium chloride (NaCl) was purchased from Merck. Hydrogen tetrachloroaurate trihydrate ($HAuCl_4 \cdot 3H_2O$) was purchased from Alfa Aesar (UK). Astralen particles were produced by thermal vaporization of graphite anode by an arc discharge using special conditions of vaporization, extraction and subsequent treatment of the cathode deposit.[30] Graphite powder produced from pulverized Alpha Aesar graphite rod (99%) was used. After chemical modification the surface of the astralen particles contained sulfa and hydroxide groups in the ionized state and was negatively charged at neutral pH. Therefore the astralen nanoparticles were dispersible in water. Zeta potential of the astralen particles was measured to be -11 ± 5 mV. Silica microspheres (diameter 3.5 μm) were purchased from Bangs Laboratories Inc (USA). Deionized water was obtained using Vodoley water treatment system (NPP Himelektronika, Russia) or Millipore Milli-Q purification system (Millipore Milli-Q, USA).

Fabrication of the SERS satellites. Silica microparticles (1 mg/ml) were coated with $(PAH/astralen)_3$ shell by the layer-by-layer (LbL) manner using aqueous PAH solutions (1 mg/ml) and astralen water dispersion (0.1 mg/ml) according to the protocol described elsewere.[44,45] At the next step, an additional layer of metal (silver or gold) was deposited on the surface by chemical reduction on the surface of the coated microspheres. The modification of the microsphere surface by silver was carried out on two stages using a well-known «silvered mirror» reaction. First, 10 μl of silver nitrate solution (0.01 M, reagent grade) and 10 μl of L-ascorbic acid solution (0.1 M, reagent grade) were added to 1 ml of dilute suspension of the LbL coated microspheres. The mixture was carefully shaken, and then 100 μl of silver nitrate was added. The color of the microsphere suspension was switched to less transparent due to silver coating on the particle surface. The obtained metal-coated microspheres were washed 5 times with water by centrifugation (6000 rpm, 20 sec) followed by re-dispersion. The modification of the microspheres by a gold layer was made using two-stage protocol previously reported for silica/gold nanoshell synthesis.[46] So-called growth solution was prepared by adding of 50 mg K_2CO_3 to 100 ml of water followed by addition of 3 ml of 1% $HAuCl_4$ solution. For the preparation of gold seeds, 220 μl of 1 M aqueous NaOH solution and 6 μl of 80% THPC solution were added to 20 ml of water. The obtained solution was vigorously agitated on a magnetic stirrer at 1000 rpm, and then 880 μl of 1% $HAuCl_4$ solution was added. The solution color was changed from yellow to brownish immediately after adding of $HAuCl_4$ solution indicating the formation of gold particles (size of about 2 nm). Then 1 ml of gold nuclei was added to 300 μl of the LbL coated microspheres. The obtained mixture has been incubated by shaking for 15 min. After centrifugation 0.5 ml of water was added to the microsphere suspension. Further 1 ml of the growth solution and 10 μl of hydrogen peroxide (3.7% water solution) were sequentially added to the microspheres decorated with gold nanoparticles (300 μl). The color of the

obtained suspension was changed from pink to blue-violet. The finally obtained particles were washed by centrifugation (6000 rpm 20 sec) followed by re-dispersion in water. Core-shell particles were transferred to PBS buffer directly before the cellular experiments.

Characterization. The prepared samples were put on electrically conductive glasses covered with ITO (indium-tin oxide) dried and investigated by SEM. The SEM images were recorded by LEO 1550 Carl Zeiss (Germany) operating at voltage of 3 kV.

Optical tweezers. The optical tweezers setup was equipped with single mode continuous-wave diode infrared lasers (Lumics LU0975M250, Germany) with wavelength of 976 nm and output power of up to 250 mW (Fig. S1). The diode laser was pigtailed by polarization-maintaining optical fiber, and the output radiation was collimated by an aspheric lens. An oil immersion objective (Olympus UPLFLN 100XOI2, Japan) with numerical aperture of 1.3 and about 60% optical transmittance at 976 nm was used for focusing the laser beam to form the optical trap. To create a maximal optical field gradient at the focal points for the most efficient trapping of micro-objects, the laser beam was expanded to the full objective aperture. The beam shifter consisting of a system of lenses placed in the confocal configuration controlled the position of the optical trap in the sample area by moving the first lens perpendicular to the beam propagation direction. The extra diode laser with the output power of 0.3 mW at wavelength of 635 nm was used to detect displacements of the trapped micro-objects. The 635 nm beam passed through the optical elements controlling the positions and the width of the beam, and then was focused into the sample chamber. The forward scattered light was collected by a 40X objective and detected using quadrant photodiodes (QPD) (Thorlabs PDQ80A, USA). Displacements of the trapped objects were extracted from the changes in the QPD photocurrent collected by an analog-to-digital-converter (National Instruments PCIe-6353, USA) working at the rate of 105 samples per second per each channel. The CCD camera was used for visual control of the trapped objects. This method is particularly sensitive for measuring displacements of the trapped spherical objects on the nanometer scale. The hermetic observation chamber was made of micro-objects suspension placed between two coverslips separated by a gap of about 0.15 mm. The observation chamber was placed on the two-coordinate motorized stage for fine sample positioning in the focal plane.

Raman Spectroscopy. Raman confocal microscope (CRM200, WITec, Ulm, Germany) equipped with a piezo-scanner (P-500, Physik Instrumente, Karlsruhe, Germany) and a diode-pumped 785 nm NIR laser excitation (Toptica Photonics AG, Graefelfing, Germany) was used in this study. The laser beam was focused through a 60× water immersion microscope objective (Nikon, NA = 1.0). The spectra were acquired with a thermoelectrically cooled CCD detector (DU401ABV, Andor, UK) behind a grating (300 g mm−1) spectrograph (Acton, Princeton Instruments Inc., Trenton, NJ, USA) with a spectral resolution of 6 cm^{-1}. For imaging integration time of 0.5 s per pixel was used. The ScanCtrlSpectroscopyPlus software (version 1.38, Witec) and WITec Project Plus (version 2.02, Witec) were used for measurement and for spectra processing, respectively. Calculated single spectra were exported into the OPUS software package (version 6.0).

In vitro cell cultivation. Mouse fibroblasts (L929 cell line) were cultivated in Dulbecco's modified Eagle medium (DMEM) supplemented with 10% fetal bovine serum (GIbco) in culture flasks (25 cm^2) in a CO_2-incubator in 5% of CO_2 atmosphere at 37°C. The medium was replaced and the cells were reseeded every 2–4 days.

Acknowledgements

DV acknowledges Alexander von Humboldt Foundation for support (Sofja Kovalevskaja Program). The work was partially supported by RFBR, research project No. 12-03-33088 mol_a_ved and research project No. 14-02-31089 mol_a, grants of the Russian Scientific Foundation (project no. 14-13-01167), Government of the Russian Federation (grant №14.Z50.31.0004), DAAD A/12/86694. The authors thank Rona Pitschke for SEM measurements. We also are grateful to Roman Schuetz for help in Raman experiments and Thomas Paulraj for help with cell staining and imaging. We want to acknowledge Andrey N. Ponomarev, Head of Science & Technical Center of Applied Researches (St-Petersburg, Russia) for providing the astralen nanoparticles for this study.

Notes and references

[a] Saratov State University, 410012, Saratov, Russia
[b] Fraunhofer Institute for Cell Therapy and Immunology, Branch Bioanalytics and Bioprocesses (Fraunhofer IZI-BB), 14476 Potsdam-Golm, Germany
[c] Max Planck Institute of Colloids and Interfaces Potsdam-Golm, Germany
[d] Lomonosov Moscow State University, Faculty of Physics 119991, Moscow, Russia
[e] Shemyakin-Ovchinnikov Institute of Bioorganic Chemistry, RAS, 117997, Moscow, Russia
[f] Institute of Biochemistry and Physiology of Plants and Microorganisms RAS, 410049 Saratov, Russia
[g] Queen Mary University of London, London, E1 4NS, United Kingdom

Electronic Supplementary Information (ESI) available: [details of any supplementary information available should be included here]. See DOI: 10.1039/c000000x/

1. D. Wang and S. Bodovitz, *Trends in Biotechnology*, 2010, **28**, 281-290.
2. F. S. O. Fritzsch, C. Dusny, O. Frick and A. Schmid, in *Annual Review of Chemical and Biomolecular Engineering, Vol 3*, ed. J. M. Prausnitz, 2012, vol. 3, pp. 129-155.
3. T. Graf and M. Stadtfeld, *Cell Stem Cell*, 2008, **3**, 480-483.
4. K. Kleparnik and F. Foret, *Analytica Chimica Acta*, 2013, **800**, 12-21.
5. T. C. Chao and A. Ros, *Journal of the Royal Society Interface*, 2008, **5**, S139-S150.
6. M. Harz, M. Kiehntopf, S. Stockel, P. Rosch, T. Deufel and J. Popp, *Analyst*, 2008, **133**, 1416-1423.
7. C. Krafft, B. Dietzek and J. Popp, *Analyst*, 2009, **134**, 1046-1057.
8. K. Kneipp, Y. Wang, H. Kneipp, L. T. Perelman, I. Itzkan, R. R. Dasari and M. S. Feld, *Physical Review Letters*, 1997, **78**, 1667-1670.
9. R. J. Swain and M. M. Stevens, *Biochem. Soc. Trans.*, 2007, **35**, 544-549.

10. W. Xie, C. Herrmann, K. Kömpe, M. Haase and S. Schlücker, *Journal of the American Chemical Society*, 2011, **133**, 19302-19305.
11. C. Leordean, M. Potara, S. Boca-Farcau, A. Vulpoi, S. Astilean and C. Farcau, *Journal of Raman Spectroscopy*, 2014, **45**, 627-635.
12. U. Huebner, H. Schneidewind, D. Cialla, K. Weber, M. Zeisberger, R. Mattheis, R. Moeller and J. Popp, 2010.
13. W.-D. Li, J. Hu and S. Y. Chou, *Opt. Express*, 2011, **19**, 21098-21108.
14. L. Zhong, X. Zhou, S. Bao, Y. Shi, Y. Wang, S. Hong, Y. Huang, X. Wang, Z. Xie and Q. Zhang, *Journal of Materials Chemistry*, 2011, **21**, 14448-14455.
15. R. A. Alvarez-Puebla, A. Agarwal, P. Manna, B. P. Khanal, P. Aldeanueva-Potel, E. Carbó-Argibay, N. Pazos-Pérez, L. Vigderman, E. R. Zubarev, N. A. Kotov and L. M. Liz-Marzán, *Proceedings of the National Academy of Sciences*, 2011, **108**, 8157-8161.
16. A. Guerrero-Martínez, S. Barbosa, I. Pastoriza-Santos and L. M. Liz-Marzán, *Current Opinion in Colloid & Interface Science*, 2011, **16**, 118-127.
17. L. Rodríguez-Lorenzo, R. de la Rica, R. A. Álvarez-Puebla, L. M. Liz-Marzán and M. M. Stevens, *Nat Mater*, 2012, **11**, 604-607.
18. P. Sajanlal and T. Pradeep, *Nano Res.*, 2009, **2**, 306-320.
19. Z. Huang, G. Meng, Q. Huang, B. Chen, C. Zhu and Z. Zhang, *Journal of Raman Spectroscopy*, 2013, **44**, 240-246.
20. I. Yoon, T. Kang, W. Choi, J. Kim, Y. Yoo, S.-W. Joo, Q. H. Park, H. Ihee and B. Kim, *Journal of the American Chemical Society*, 2008, **131**, 758-762.
21. G. Rusciano, A. C. De Luca, A. Sasso and G. Pesce, *Analytical Chemistry*, 2007, **79**, 3708-3715.
22. M. J. Guffey and N. F. Scherer, *Nano Letters*, 2010, **10**, 4302-4308.
23. G. McNay, F. T. Docherty, D. Graham, W. E. Smith, P. Jordan, M. Padgett, J. Leach, G. Sinclair, P. B. Monaghan and J. M. Cooper, *Angewandte Chemie International Edition*, 2004, **43**, 2512-2514.
24. C. Jiang, S. Markutsya, Y. Pikus and V. V. Tsukruk, *Nat Mater*, 2004, **3**, 721-728.
25. C. Lu, H. Möhwald and A. Fery, *The Journal of Physical Chemistry C*, 2007, **111**, 10082-10087.
26. A. Yashchenok, A. Masic, D. Gorin, B. S. Shim, N. A. Kotov, P. Fratzl, H. Möhwald and A. Skirtach, *Small*, 2013, **9**, 351-356.
27. C. S. Peyratout and L. Dahne, *Angew. Chem. Int. Ed.*, 2004, **43**, 3762-3783.
28. A. L. Becker, A. P. R. Johnston and F. Caruso, *Small*, 2010, **6**, 1836-1852.
29. S. A. Sukhishvili, *Curr. Opin. Colloid Interface Sci.*, 2005, **10**, 37-44.
30. A. I. Shames, E. A. Katz, A. M. Panich, D. Mogilyansky, E. Mogilko, J. Grinblat, V. P. Belousov, I. M. Belousova and A. N. Ponomarev, *Diamond and Related Materials*, 2009, **18**, 505-510.
31. R. Stiufiuc, C. Iacovita, C. Lucaciu, G. Stiufiuc, A. Dutu, C. Braescu and N. Leopold, *Nanoscale Research Letters*, 2013, **8**, 47.
32. I. Y. Stetciura, A. V. Markin, A. N. Ponomarev, A. V. Yakimansky, T. S. Demina, C. Grandfils, D. V. Volodkin and D. A. Gorin, *Langmuir*, 2013, **29**, 4140-4147.
33. A. Gutés, R. Maboudian and C. Carraro, *Langmuir*, 2012, **28**, 17846-17850.
34. T. Paulraj, N. Feoktistova, N. Velk, C. Duschl and D. Volodkin, *Macromol. Rapid Comm.*, 2014, **35** (16), 1408-13..
35. K. Uhlig, N. Madaboosi, S. Schmidt, M. S. Jager, J. Rose, C. Duschl and D. V. Volodkin, *Soft Matter*, 2012, **8**, 11786-11789.
36. R. Weissleder, *Nat. Biotech*, 2001, **19**, 316-317.
37. D. Volodkin, R. von Klitzing, H. Moehwald, Polyelectrolyte multilayers: towards single cell studies, *Polymers*, 2014, **6** (5), 1502-1527.
38. Volodkin, D.; Skirtach, A.; Möhwald, H., LbL Films as Reservoirs for Bioactive Molecules Bioactive Surfaces. Börner, H. G.; Lutz, J.-F., Eds. Springer Berlin / Heidelberg: 2011; Vol. 240, pp 135-161.
39. Volodkin, D.; Skirtach, A.; Möhwald, H., Bioapplications of light-sensitive polymer films and capsules assembled using the layer-by-layer technique. *Polym Int* 2012, **61** (5), 673-679.
40. Skirtach, A. G.; Volodkin, D. V.; Mohwald, H., Bio-interfaces-Interaction of PLL/HA Thick Films with Nanoparticles and Microcapsules. *ChemPhysChem* 2010, **11** (4), 822-829.
41. Volodkin, D., CaCO3 templated micro-beads and -capsules for bioapplications. *Advances in Colloid and Interface Science* 2014**,** *206*, 437-454.
42. Schmidt, S.; Volodkin, D., Microparticulate biomolecules by mild CaCO3 templating. *J Mater Chem B* 2013, **1** (9), 1210-1218.
43. H. Chen, C. Wang, Y. Lou, *IEEE Trans. Biomed. Engineering, 2013,* **60**, 1518-1527.
44. R. K. Iler, *Journal of Colloid and Interface Science*, 1966, **21**, 569-594.
45. G. Decher, J. D. Hong and J. Schmitt, *Thin Solid Films*, 1992, **210–211, Part 2**, 831-835.
46. B. E. Brinson, J. B. Lassiter, C. S. Levin, R. Bardhan, N. Mirin and N. J. Halas, *Langmuir*, 2008, **24**, 14166-14171.